Oxalate and 2,2′-bipyrimidine as bis-chelating ligands in the honeycomb layered compound $\{[Fe_2(bpym)(ox)_2]\cdot 5H_2O\}_n$

Donatella Armentano,[a] Giovanni de Munno,*[a] Francesc Lloret,[b] Miguel Julve,*[b] Jacques Curély,[c] Amy M. Babb[d] and Jack Y. Lu[d]

[a] *Dipartimento di Chimica, Università degli Studi della Calabria, 87030, Arcavacata di Rende, Cosenza, Italy*
[b] *Departament de Química Inorgànica/Instituto de Ciencia Molecular, Facultat de Química de la Universitat de València, Dr. Moliner 50, 46100, Burjassot, València, Spain. E-mail: miguel.julve@uv.es*
[c] *Centre de Physique Moléculaire Optique et Hertzienne, Université Bordeaux I, 351 Cours de la Libération, 33405, Talence Cédex, France*
[d] *Department of Chemistry, University of Houston-Clear Lake, Houston, TX 77058, USA*

Received (in Montpellier, France) 23rd July 2002, Accepted 26th September 2002
First published as an Advance Article on the web 28th November 2002

The novel two-dimensional iron(II) compound of formula $\{[Fe_2(bpym)(ox)_2]\cdot 5H_2O\}_n$ (**1**) [bpym = 2,2′-bipyrimidine and ox = oxalate dianion] is obtained by reaction of oxalic acid, iron(II) chloride and 2,2′-bipyrimidine in aqueous solution. The structure of **1** is made up of oxalato-bridged iron(II) chains cross-linked by bischelating bpym affording a honeycomb lattice. Variable-temperature magnetic susceptibility data of **1** show the occurrence of relatively large antiferromagnetic interactions between the high spin iron(II) ions separated by more than 5.5 Å through bridging bpym [$J_{bpym} = -4.0(2)$ cm^{-1}] and ox [$J_{ox} = ca.\ -7.8(2)$ cm^{-1}] ligands. These values compare well with those obtained in the iron(II) chain $[Fe(dpa)(ox)]_n$ (**2**) [$J_{ox} = -8.0(2)$ cm^{-1}] (dpa = 2,2′-dipyridylamine) and dinuclear $\{[Fe(H_2O)_4]_2(bpym)\}(SO_4)_2\cdot 2H_2O$ (**3**) ($J_{bpym} = -3.4$ cm^{-1}) compounds where bischelating ox (**1** and **2**) and bpym (**1** and **3**) groups and the bidentate dpa (**2**) ligand are present.

Introduction

The first studies of complex formation between iron(II) and 2,2′-bipyrimidine (hereafter denoted bpym) revealed that more than one complex was formed depending on the ratio of bpym to iron(II).[1] A Job plot showed that the species of maximum colour intensity in aqueous solution for this system contains a 3:1 bpym to Fe(II) molar ratio. The recent structural determination and magnetic study of the $[Fe(bpym)_3]^{2+}$ species as a perchlorate salt[2] revealed that it is is a diamagnetic compound in agreement with the strong field ligand character of this bis-α-diimine type ligand. This tris-chelated cation was used as a suitable counterion to isolate the dinuclear iron(III) complexes of formula $[Fe^{II}(bpym)_3]_2[Fe^{III}_2(ox)_5]\cdot 8H_2O$[3] (ox = oxalate dianion) and $[Fe^{II}(bpym)_3]_2[Fe^{III}_2(N_3)_{10}]\cdot 2H_2O$[4] which exhibit significant antiferro- (through bridging oxalato) and ferromagnetic (through double end-on azido bridges) interactions between the iron(III) ions. The bis-chelating coordination ability of bpym also makes possible the use of the $[Fe(bpym)_3]^{2+}$ unit as a ligand attached to metal ions such as in the neutral trinuclear $[Fe^{II}(bpym)_3Na(H_2O)_2Fe^{III}(ox)_3]\cdot 4H_2O$[3] complex where one of the three bpym groups acts as a bridge between iron(II) and sodium(I).

From a magnetic point of view, a more interesting situation arises when lowering the number of bpym ligands coordinated to iron(II). So, this metal ion becomes high spin ($S = 2$) in the dinuclear $[Fe_2(bpym)_3X_4]$ (X = NCS and Cl)[5,6] and chain $[Fe(bpym)(NCS)_2]_n$[7] compounds. Variable-temperature magnetic suscepibility measurements show the occurrence of a relatively large antiferromagnetic interaction between the high spin iron(II) ions separated by more than 5.9 Å through bridging bpym in the dimer ($J = -4.1$ cm^{-1} with X = NCS$^-$, the Hamiltonian being $\hat{H} = -J\hat{S}_A\cdot\hat{S}_B$) and in the chain ($J = -3.5$ cm^{-1}, $\hat{H} = -J\sum_i \hat{S}_i\cdot\hat{S}_{i+1}$) complexes. This high spin state for the iron(II) center is kept in the bpym-bridged dinuclear iron(II) species $[Fe_2(bpym)(H_2O)_8]^{4+}$ which is readily isolated in the open air as a sulfate salt from aqueous solutions containing iron(II) sulfate and bpym in a 2:1 molar ratio.[8] Four terminally bound water molecules and two bpym-nitrogen atoms build a distorted octahedral environment around the iron atom. The easy replacement of these coordinated water molecules by anionic bridging ligands makes this highly positively charged species a suitable precursor of higher dimensionality systems. In this respect, the reaction of $[Fe_2(bpym)(H_2O)_8]^{4+}$ with azide and dicyanamide (dca) afforded two-dimensional compounds of formulae $[Fe_2(bpym)(N_3)_4]_n$,[9] $[Fe_2(bpym)(dca)_4]\cdot H_2O$[10] and $[Fe_2(bpym)(dca)_4(H_2O)_2]$.[10] The azide-containing complex has a honeycomb layered structure with alternating intralayer antiferro- (through bridging bpym) and ferromagnetic (through the double end-on azide bridges) magnetic interactions between the high spin iron(II) ions. In the case of the dca derivatives, bis-bidentate bpym and dca ligands adopting the end-to-end bridging mode lead to sheet-like polymers whose magnetic behaviour is similar to that of an isolated bpym-bridged pair of high spin iron(II) ions.

In the present work, we present the preparation, crystal structure and magnetic study of the two-dimensional compound $\{[Fe_2(bpym)(ox)_2]\cdot 5H_2O\}_n$ (**1**) where intralayer antiferromagnetic interactions between high spin iron(II) ions through bridging bpym and oxalato groups occur. The magnetic properties of the oxalato-bridged iron(II) chain $[Fe(dpa)(ox)]_n$ (**2**) (dpa = 2,2′-dipyridylamine)[11] and the bpym-bridged

iron(II) dinuclear complex $\{[Fe(H_2O)_4]_2(bpym)\}(SO_4)_2\cdot 2H_2O$ (**3**)[8] are also included for comparison. The structures of **2** and **3** and the magnetic properties of **3** were reported elsewhere.[8,11]

Experimental

Materials

Iron(II) chloride, oxalic acid dihydrate and bpym were purchased from commercial sources and used as received. $[Fe(dpa)(ox)]_n$ (**2**) and $\{[Fe(H_2O)_4]_2(bpym)\}(SO_4)_2\cdot 2H_2O$ (**3**) were prepared as previously described.[8,11] Elemental analyses (C, H, N) were carried out by the Microanalytical Service of the Università degli Studi della Calabria.

Preparation of $\{[Fe_2(bpym)(ox)_2]\cdot 5H_2O\}_n$ (1). Oxalic acid (6 mmol) was added under continuous stirring to an aqueous solution (50 cm^3) containing a mixture of iron(II) chloride (6 mmol) and bpym (3 mmol). The resulting brown solution was allowed to evaporate at room temperature. Brown plates of **1** suitable for X-ray diffraction were formed after several days. They were collected by filtration and washed with ethanol and diethyl ether. Yield about 60%. Anal. calc. for $C_{12}H_{16}Fe_2N_4O_{13}$ (**1**): C, 26.89; H, 3.01; N, 10.45. Found: C, 26.70; H, 3.10; N, 10.33%. The infrared spectrum of **1** reveals the presence of bis-chelating bpym [asymmetric doublet at 1580vs and 1550w cm^{-1} (ring stretching vibrations of bpym)][7,8,12] and oxalato [absorptions at 1670vs (ν_{as}(O–CO)), 1355 m and 1307s cm^{-1} (ν_s(O–C–O))][13] as well as a strong and broad absorption centered at *ca.* 3470 cm^{-1} due to the presence of hydrogen bonded water molecules.[14]

Physical techniques

IR spectrum of **1** (4000–400 cm^{-1}) was recorded on a Bruker IF S55 spectrophotometer with a sample prepared as a KBr pellet. Variable-temperature [5.0–290 (**1**) and 2.0–300 K (**2**)] magnetic susceptibility measurements on polycrystalline samples of **1** and **2** were carried out with a Quantum Design SQUID operating at 5000 Oe in the high temperature range (25–290 K) and at 250 Oe at $T < 25$ K in order to avoid saturation phenomena. Diamagnetic corrections for the molar units were estimated from Pascal's constants[15] as -237×10^{-6} (**1**) and -151×10^{-6} cm^3 mol^{-1} (**2**).

X-Ray data collection and structure refinement

A crystal of **1** of dimensions $0.22\times0.18\times0.06$ mm was mounted on a Bruker R3m/V automatic diffractometer and used for data collection. Diffraction data were collected at room temperature by using graphite-monochromated Mo-Kα radiation ($\lambda = 0.71073$ Å) with the ω–2θ scan method. The unit cell parameters were determined from least-squares refinement of the setting angles of 25 reflections in the 2θ range 15–30. A summary of the crystallographic data and of the structure refinement is given in Table 1. Examination of two standard reflections, monitored after every 50 reflections, showed no sign of crystal deterioration. Lorentz-polarization and Ψ-scan absorption corrections[16] were applied to the intensity data. The maximum and minimum transmission factors were 0.728 and 0.913.

The structure of **1** was solved by standard Patterson methods and subsequently completed by Fourier recycling. All non-hydrogen atoms were refined anisotropically except for the oxygen atom of the water molecules. The hydrogen atoms of the water molecule were not located whereas those of the bpym ligand were set in calculated positions and refined as riding atoms with a common fixed isotropic thermal parameter.

Table 1 Crystallographic data for $\{[Fe_2(bpym)(ox)_2]\cdot 5H_2O\}_n$ (**1**)

Formula	$C_{12}H_{16}Fe_2N_4O_{13}$
FW	544.04
Temperature/K	293(2)
Wavelength/Å	0.71073
Crystal system	monoclinic
Space group	$C2/m$
a/Å	9.674(3)
b/Å	16.940(4)
c/Å	6.1570(10)
β/°	101.60(2)
Volume/Å^3	988.4(4)
D_c/g cm^{-3}	1.827
Z	2
F(000)	544
μ(Mo-Kα)/cm^{-1}	15.43
θ range/deg	2.40–27.06
Index ranges	$-12\le h\le 12$
	$0\le k\le 21$
	$0\le l\le 7$
Reflections collected	1256
Independent reflections	1123 [R(int) = 0.026]
Refinement method	Full-matrix least-squares on F^2
Data/restraints/parameters	1123/0/86
Goodness-of-fit[a]	1.043
R_1/wR_2[b,c]	0.0482/0.1006
R_1/wR_2(all data)	0.0680/0.1092
Largest diff. peak/e Å^{-3}	0.437
Largest diff. hole/e Å^{-3}	−0.372

[a] Goodness-of-fit = $\{\Sigma[w(F_o^2-F_c^2)^2/(N_o-N_p)]\}^{1/2}$. [b] $I > 2\sigma(I)$. [c] $R_1 = \Sigma(|F_o|-|F_c|)/\Sigma|F_o|$, $wR_2 = \{\Sigma[w(F_o^2-F_c^2)^2]/\Sigma[w(F_o^2)^2]\}^{1/2}$ and $w = 1/[\sigma^2(F_o^2)+(aP)^2+bP]$ with $P = [F_o^2+2F_c^2]/3$, $a = 0.0412$ and $b = 3.0615$.

The final full-matrix least-squares refinement on F^2, minimizing the function $\Sigma w(|F_o|-|F_c|)^2$, reached convergence with values of the discrepancy indices given in Table 1. Solutions and refinements were performed with the SHELXTL NT system.[17] The final geometrical calculations were carried out with the PARST program.[18] The drawings were performed using the XP utility of the SHELXTL NT system. Interatomic bond distances and angles for **1** are listed in Table 2.

The space group of **1** cannot be uniquely determined from the systematic absences, which only indicate the presence of a *C*-centered cell: the choice is between the acentric $C2$ or Cm groups and the centric $C2/m$ one. The latter was favoured

Table 2 Interatomic bond lengths (Å) and angles (°) for compound **1**[a,b]

Fe(1)–O(1)	2.101(3)	Fe(1)–O(2)	2.126(3)
Fe(1)–N(1)	2.191(3)	O(1)–C(2)	1.246(4)
O(2)–C(2b)	1.253(4)	N(1)–C(1)	1.333(4)
N(1)–C(3)	1.344(5)	C(1)–C(1c)	1.484(9)
C(2)–C(2b)	1.553(7)	C(3)–C(4)	1.376(5)
O(1)–Fe(1)–O(1c)	171.9(1)	O(1)–Fe(1)–O(2c)	96.3(1)
O(1c)–Fe(1)–O(2c)	78.3(1)	O(2c)–Fe(1)–O(2)	97.1(1)
O(1)–Fe(1)–N(1)	97.9(1)	O(1c)–Fe(1)–N(1)	88.5(1)
O(2c)–Fe(1)–N(1)	163.0(1)	O(2)–Fe(1)–N(1)	95.0(1)
N(1)–Fe(1)–N(1c)	76.1(1)	C(2)–O(1)–Fe(1)	114.9(2)
C(2b)–O(2)–Fe(1)	113.7(2)	C(1)–N(1)–C(3)	116.7(3)
C(1)–N(1)–Fe(1)	114.9(2)	C(3)–N(1)–Fe(1)	128.4(2)
N(1a)–C(1)–N(1)	125.8(4)	N(1)–C(1)–C(1c)	117.1(2)
O(1)–C(2)–O(2b)	126.9(3)	O(1)–C(2)–C(2b)	116.4(4)
O(2)–C(2)–C(2b)	116.7(4)	N(1)–C(3)–C(4)	121.5(4)
C(3)–C(4)–C(3a)	117.7(5)		

[a] Estimated standard deviations in the last significant digits are given in parentheses. [b] Symmetry transformations to generate equivalent atoms: (a) = x, $-y+1$, z; (b) = $-x+1/2$, $-y+3/2$, $-z$; (c) $-x+1$, y, $-z$.

by the intensities statistics, and consequently, the structure solution and refinement were carried out in the centrosymmetric space group. The analysis of the residual electronic density in a final difference-Fourier map revealed three distinct peaks [two, O(4) and O(5), in general positions and one, O(3), in a special position on a twofold axis], which could be interpreted as crystallization water molecules. The elemental analysis indicated a 5:2 water to iron molar ratio. Five oxygen atoms of the water molecules may be obtained by applying the twofold axis operation to the three peaks, while ten positions are obtained when the mirror operation is also applied. Then, we tried to refine the structure of **1** in *C*2 and *Cm*, but all our attempts gave worse results with large correlations between atomic positional parameters. Therefore, the refinement was completed in $C2/m$ by assuming a disordered position of the water molecules in which ten half oxygen atoms are arranged as two staggered five-membered rings.

CCDC reference number 189567 (**1**). See http://www.rsc.org/suppdata/nj/b2/b207241f/ for crystallographic data in CIF or other electronic format.

Results and discussion

Description of the structure of 1

The structure of **1** is made up of parallel neutral sheets each one consisting of an infinite hexagonal array of iron(II) ions bridged by bisbidentate oxalate and bpym ligands (Fig. 1). The iron atom exhibits a distorted six-coordinated FeN_2O_4 chromophore. The reduced values of the angles subtended at the iron atom by the bischelating bpym [76.1(1)° for N(1)–Fe(1)–N(1c)] and ox [78.3(1)° for O(1)–Fe(1)–O(2)] ligands are the main factors accounting for this distortion.

Five uncoordinated water molecules are hosted in each hole of the sheetlike polymer forming a planar five-membered ring [the maximum deviation from the mean plane is 0.075(1) Å at O(5)] (Fig. 1 and 2). They are linked together by means of hydrogen bonds within the ring [2.89(2), 2.95(3) and 2.62(3) Å for O(4)···O(3), O(5)···O(4) and O(5)···O(5i), respectively; (i) = $2-x$, y, $1-z$], between adjacent rings [2.69(2) for O(4)···O(4g); (g) = $-x$, y, $-z+2$] and between the ring and the wall of the channel [2.913(6) Å for O(3)···O(2r) and O(3)···O(2c) and 2.86(2) Å for O(5)···O(2t); (r) = $x+1/2$, $y+1/2$, $z-1$, (s) = $-x+1/2$, $y+1/2$, $-z$ and (t) = $x+1/2$, $-y+3/2$, $z-1$]. These hydrogen bonds contribute to the stabilization of the two-dimensional structure.

Compound **1** is isostructural to the parent copper(II) complex of formula $\{[Cu_2(bpym)(ox)_2]\cdot 5H_2O\}_n$ (**4**)[19] and similar to both the homometallic manganese(II) compound $\{[Mn_2(bpym)(ox)_2]\cdot 6H_2O\}_n$ (**5**)[20] and the heterometallic Cr(III)–Na(I) complex $\{[NaCr(bpym)(ox)_2]\cdot 5H_2O\}_n$ (**6**).[21] The values of the bond distances around the iron atom are somewhat longer than those observed in **4** but shorter than in **5** in agreement with the decrease of the ionic radius when going from Mn(II) to Cu(II): the average values of the Fe–O(ox) and Fe–N(bpym) equatorial bonds in **1** are 2.126(3) and 2.191(3) Å whereas the corresponding bonds in the parent Cu(II) and Mn(II) derivatives are 2.086(3) and 2.129(3) Å (**4**) and 2.160(2) and 2.283(2) Å (**5**). Analogously, the average Fe–O(ox) axial distance [2.101(3) Å] is comprised between those of compounds **4** [2.076(3) Å] and **5** [2.156(2) Å]. As a consequence of the geometrical variations around the metal atom, larger hexameric rings occur in **1** with respect to **4** and smaller with respect to **5**. The bpym and ox ligands in **1** are planar and they form a dihedral angle of 80.2(1)°. The values of the bond lengths and angles within these ligands are in agreement with those reported in the literature. The intra-ring carbon–carbon bond distance in bpym [1.376(5) Å] is significantly shorter than the carbon–carbon bond length in the oxalate ligand [1.553(7) Å]. The iron atom is slightly shifted from the bpym and ox planes [0.025(1) and 0.050(5) Å, respectively]. As shown in Fig. 1, the two-dimensional polymer grows in the xy plane and it is formed by repeating almost circular hexanuclear rings. The intra-ring iron–iron distances are 5.824(1) [Fe(1)···Fe(1a)], 5.513(1) [Fe(1)···Fe(1b)], 9.754(2) [Fe(1)···Fe(1f)], 9.674(3) [Fe(1)···Fe(1d)], 11.292(2) [Fe(1)···Fe(1e)] and 11.116(2) Å [Fe(1f)···Fe(1b)]. The plane of the five-membered ring of the water molecules makes dihedral angles with the planes of bpym and ox of 14.5(3) and 70.7(2)°, respectively. Graphite-like interactions between the bpym ligands of adjacent layers of the polymer occur [the separation between bpym planes of neighbouring layers is 3.549(3) Å].

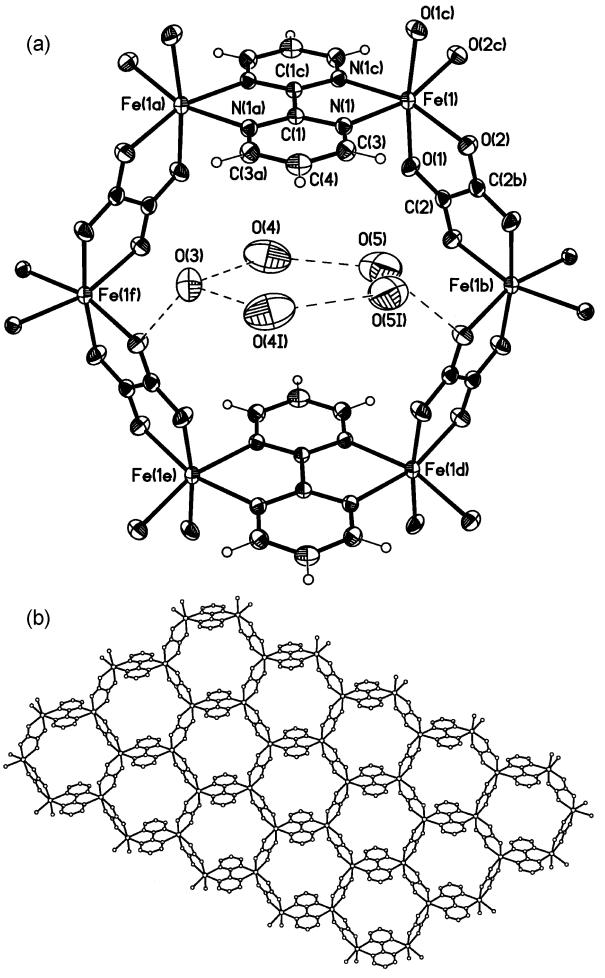

Fig. 1 View of the structure of **1** (thermal ellipsoids are drawn at the 30% probability level): (top) hexameric repeating unit with the labelling scheme; (bottom) a sheet extending in the xy plane that shows the chicken-wire arrangement adopted by the iron atoms (hydrogen atoms and water molecules have been omitted for the sake of clarity). Symmetry code: (a) x, $-y+1$, z; (b) $-x+1/2$, $-y+3/12$, $-z$; (c) $-x+1$, y, $-z$; (d) $x-1$, y, z; (e) $x+1$, $-y+1$, z; (f) $x-1/2$, $y-1/2$, z.

Finally, it deserves to be noted that the honeycomb layered structure of **1**, also observed in compounds **4**–**6**, is dictated by the occurrence of regularly alternating tris-chelated units of opposite chirality in each layer. This feature was previously observed by other authors when using the tris-chelated $[M^{III}(ox)_3]^{3-}$ unit as a building block in designing honeycomb layered stuctures of formula $[M^{II}M^{III}(ox)_3]_n^{n-}$ where M^{II} = V, Cr, Mn, Fe, Co, Ni, Cu and Zn and M^{III} = V, Cr and Fe.[22] Both families have the same honeycomb layered arrangement of metal ions, but the former one (compounds **1** and **4**–**6**) deals with neutral species and the latter requires specific cations of the type XR_4^+ (X = N, P; R = alkyl or aryl groups)[23,24] or ferrocenium.[25]

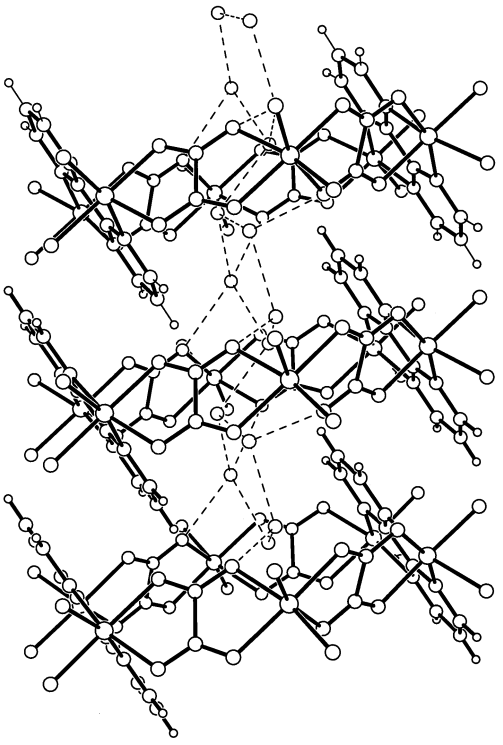

Fig. 2 Side view of three adjacent layers showing the intercalation of the five-membered rings of water molecules.

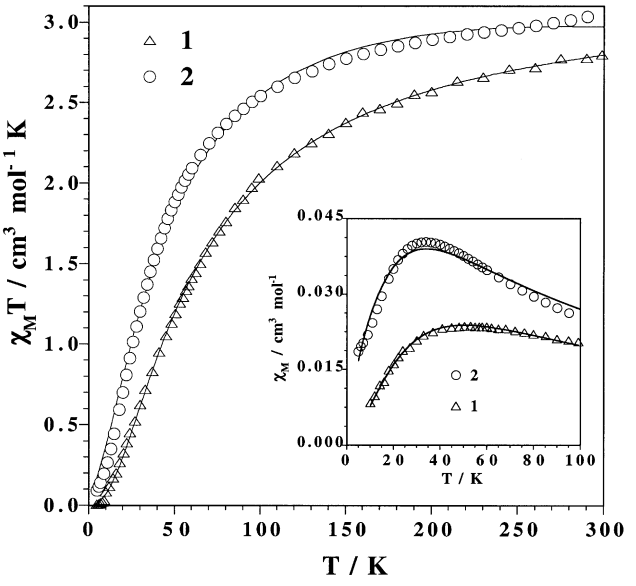

Fig. 3 $\chi_M T$ *vs.* T plot for complexes **1** and **2**: (△, ○) experimental data; (—) best-fit curves (see text). The inset shows the χ_M *vs.* T plot in the vicinity of the maximum.

Magnetic properties of 1 and 2

The temperature dependence of $\chi_M T$ for **1** [χ_M is the magnetic susceptibility per one Fe(II) ion] is shown in Fig. 3. At room temperature, $\chi_M T$ is 2.80 cm^3 mol^{-1} K, a value which is somewhat below that calculated for a magnetically non-interacting spin quintet through the spin-only formula [$\chi_M T = 3$ cm^3 mol^{-1} K with $g = 2.0$]. $\chi_M T$ for **1** monotonically decreases from room temperature to practically vanish at very low temperatures and the susceptibility curve shows a maximum at 53 K (see inset of Fig. 3). These features indicate the occurrence of relatively strong intralayer antiferromagnetic interactions between the high spin iron(II) ions. Given that both bpym[5,7–10,26,27] and oxalate[28] ligands are able to mediate large antiferromagnetic interactions when acting as bridges between paramagnetic centers, it is thus clear that the magnetic behaviour of compound **1** is that of an alternating magnetic plane with antiferromagnetic interactions through bpym and ox groups. Consequently, we have analysed the magnetic data of **1** through the expression derived recently for a two-dimensional Heisenberg classical honeycomb lattice,[29] the involved quantum spins in the present case ($S_{Fe^{II}} = 2$) being assimilated to classical ones. Best-fit parameters are: $J_{ox} = -7.8(2)$ cm^{-1}, $J_{bpym} = -4.0(2)$ cm^{-1} and $g = 2.20(2)$. Although the computed curve does not match very well the magnetic data in the vicinity of the maximum of susceptibility (see inset of Fig. 3), the values of the magnetic interactions obtained are correct in sign and its size is physically reasonable (see below). The mismatch between the calculated curve and the experimental data is due to the orbital contribution of the octahedral high spin iron(II) ion [$^4T_1$ ground state]. The low symmetry of the tris-chelated iron(II) ion in **1** [C_2 symmetry] is not enough to totally quench the orbital contribution of the ground state.

In order to check the validity of the values of the magnetic interactions found through bridging bpym and ox ligands in **1**, one needs to compare them with those found in lower nuclearity compounds of high spin iron(II) having these bridges and the same FeN_2O_4 chromophore.[30] A suitable example for the bpym case is provided by the dinuclear {[Fe(H$_2$O)$_4$]$_2$(bpym)}(SO$_4$)$_2$·2H$_2$O (**3**)[8] compound where four coordinated water molecules play the role of the four oxalate-oxygens in **1**. It is very satyisfying to see that the value of the magnetic coupling through bridging bpym in **3** ($J = -3.4$ cm^{-1}) agrees well with that found in **1**, the iron–iron separation across bridging bpym being practically identical [5.824(1) Å in **1** *versus* 5.836(1) Å in **3**].

As far as the oxalato bridge is concerned, the values of the magnetic coupling between high spin iron(II) ions in the structurally characterized chain [Fe(ox)(H$_2$O)$_2$]$_n$ ($J = -8.8$ cm^{-1})[13c] correspond to a FeO_6 chromophore. The recent structural report on the oxalato-bridged iron(II) chain [Fe(dpa)(ox)]$_n$ (**2**)[11] prompted us to investigate its magnetic properties in order to use them as a suitable model for the oxalato framework of compound **1**. A bidentate dpa ligand and two oxalate groups define a FeN_2O_4 chromophore around each iron atom in **2**. The magnetic properties of **2** in the form of $\chi_M T$ *versus* T plot are shown in Fig. 3. $\chi_M T$ at room temperature is 3.04 cm^3 mol^{-1} K, a value which is in agreement with the occurrence of a high spin iron(II) ion in **2**. This value exhibits a continuous decrease upon cooling to practically vanish at 2 K. The susceptibility curve exhibits a maximum at 34 K (see inset of Fig. 3) revealing that a significant intrachain antiferromagnetic interaction between high spin iron(II) ions occurs in **2**. Our attempts to reproduce theoretically the susceptibility data of **2** by using the classical spin Heisenberg chain model[31] through the Hamiltonian $\hat{H} = -\sum_i J \hat{S}_i \cdot \hat{S}_{i+1}$ with $S_i = S_{i+1} = 2$ reproduce the position of the maximum but not its height. The best-fit parameters are: $J = -8.0(2)$ cm^{-1} and $g = 2.25(2)$. The consideration of a parameter accounting for the interchain interactions did not improve significantly the quality of the fit. Most likely, the orbital contribution associated with the six coordinated high spin iron(II) in **2** is at the origin of this mismatch between the computed and experimental data in the vicinity of the susceptibility maximum. Anyway, the value of the antiferromagnetic coupling in **2** is quite close to that found for J_{ox} in **1** (−7.8(2) cm^{-1}) and this is not surprising because the iron atoms have the same chromophore in **1** and **2** and their separation across the bridging oxalato group is nearly identical [5.513(1) and 5.545(1) Å in **1** and **2**, respectively].

Finally, we would like to finish the present contribution with a brief comment of how the position of the maximum of the magnetic susceptibility for the compounds **1**–**3** is governed by the strength of the antiferromagnetic interaction across the bpym (compound **3**) and ox (compound **2**) bridges and also by a combination of both of them (compound **1**). The shift of the position of the susceptibility maximium towards higher temperatures when going from **3** to **1** [T_{max} = 15.1 (**3**), 34 (**2**) and 53 K (**1**)] reflects the greater efficiency of the oxalate in mediating antiferromagnetic interactions when compared to bpym and also the fact that both bridges are involved in compound **1**. In the near future, we will try to extend these studies to other divalent first row transition metal ions.

Acknowledgements

This work was supported by the Ministerio Español de Ciencia y Tecnología (Project BQU2001-2928), the Itialian Ministery of Research and Education, the TMR Programme of the European Union (Contract ERBFMRXCT98-0181) and the Welch Foundation.

References

1 D. B. Blye and M. G. Mellon, *Anal. Chem.*, 1963, **35**, 1386.
2 G. De Munno, M. Julve and J. A. Real, *Inorg. Chim. Acta*, 1997, **255**, 185.
3 D. Armentano, G. De Munno, J. Faus, F. Lloret and M. Julve, *Inorg. Chem.*, 2001, **40**, 655.
4 G. De Munno, T. Poerio, G. Viau, M. Julve and F. Lloret, *Angew. Chem., Int. Ed. Engl.*, 1997, **36**, 1459.
5 J. A. Real, J. Zarembowitch, O. Kahn and X. Solans, *Inorg. Chem.*, 1987, **26**, 2939.
6 J. S. Sun, H. Zhao, X. Ouyang, R. Clérac, J. A. Smith, J. M. Clemente-Juan, C. Gómez-García, E. Coronado and K. Dunbar, *Inorg. Chem.*, 1999, **38**, 5841.
7 G. De Munno, M. Julve, J. A. Real, F. Lloret and R. Scopelliti, *Inorg. Chim. Acta*, 1996, **250**, 81.
8 E. Andrés, G. De Munno, M. Julve, J. A. Real and F. Lloret, *J. Chem. Soc., Dalton Trans.*, 1993, 2169.
9 G. De Munno, T. Poerio, G. Viau, M. Julve, F. Lloret, Y. Journaux and E. Rivière, *Chem. Commun.*, 1996, 2587.
10 S. Triki, F. Thétiot, J. R. Galán-Mascarós, J. Sala Pala and K. R. Dunbar, *New J. Chem.*, 2001, **25**, 954.
11 J. Y. Lu, T. J. Schroeder, A. M. Babb and M. Olmstead, *Polyhedron*, 2001, **20**, 2445.
12 M. Julve, M. Verdaguer, G. De Munno, J. A. Real and G. Bruno, *Inorg. Chem.*, 1993, **32**, 795.
13 (*a*) N. F. Curtis, *J. Chem. Soc. A*, 1968, 1584; (*b*) N. F. Curtis, *J. Chem. Soc.*, 1963, 4109; (*c*) J. T. Wrobleski and D. B. Brown, *Inorg. Chem.*, 1979, **18**, 2738.
14 K. Nakamoto, *Infrared and Raman Spectra of Inorganic and Coordination Compounds*, 4th edn., Wiley, New York, 1986, p. 227.
15 A. Earnshaw, *Introduction to Magnetochemistry*, Academic Press, London and New York, 1968.
16 A. C. T. North, D. C. Philips and F. S. Matews, *Acta Crystallogr., Sect. A*, 1968, **24**, 351.
17 SHELXTL NT, Version 5.10, Bruker Analytical X-ray Instruments Inc., Madison, WI, 1998.
18 M. Nardelli, *Comput. Chem.*, 1983, **7**, 95.
19 G. De Munno, M. Julve, F. Nicolò, F. Lloret, J. Faus, R. Ruiz and E. Sinn, *Angew. Chem., Int. Ed. Engl.*, 1993, **32**, 795.
20 G. De Munno, R. Ruiz, F. Lloret, J. Faus, R. Sessoli and M. Julve, *Inorg. Chem.*, 1995, **34**, 408.
21 G. De Munno, D. Armentano, M. Julve, F. Lloret, R. Lescouëzec and J. Faus, *Inorg. Chem.*, 1999, **38**, 2234.
22 S. Decurtins, H. W. Schmalle, R. Pellaux, P. Fischer and A. Hauser, *Mol. Cryst. Liq. Cryst.*, 1997, **305**, 227.
23 R. Pellaux, H. W. Schmalle, R. Huber, P. Fischer, T. Hauss, B. Ouladdiaf and S. Decurtins, *Inorg. Chem.*, 1997, **36**, 2301.
24 C. Mathonière, C. J. Nuttall, S. G. Carling and P. Day, *Inorg. Chem.*, 1996, **35**, 1201.
25 E. Coronado, J. R. Galán-Mascarós, C. J. Gómez-García, J. Ensling and P. Gütlich, *Chem. Eur. J.*, 2000, **6**, 552.
26 J. Sletten, H. Daraghmeh, F. Lloret and M. Julve, *Inorg. Chim. Acta*, 1998, **279**, 1998.
27 G. De Munno and M. Julve, in *Metal Ligand Interactions. Structure and Reactivity*, eds. N. Russo and D. R. Salahub, Kluwer, Dordrecht, 1996, vol. 474, p. 139 and references therein.
28 O. Kahn, *Molecular Magnetism*, VCH, Weinheim, 1993.
29 J. Curély, F. Lloret and M. Julve, *Phys. Rev. B*, 1998, **58**, 11 465.
30 P. Román, C. Guzmán-Miralles, A. Luque, J. I. Beitia, J. Cano, F. Lloret, M. Julve and S. Alvarez, *Inorg. Chem.*, 1996, **35**, 3741.
31 M. E. Fisher, *Am. J. Phys.*, 1964, **32**, 343.